Department of Veterans Affairs

Journal of Rehabilitation Research and Development Vol. 38 No. 1, January/February 2001
Pages 41–55

Dynamic calibration of a wheelchair dynamometer

Carmen P. DiGiovine, MS; Rory A. Cooper, PhD; Michael L. Boninger, MD
Human Engineering Research Laboratories, VA Rehabilitation Research and Development Center, VA Pittsburgh Healthcare System, Pittsburgh, PA; Departments of Rehabilitation Science and Technology, Bioengineering, Physical Medicine and Rehabilitation, and Mechanical Engineering, University of Pittsburgh, Pittsburgh, PA

Abstract—The inertia and resistance of a wheelchair dynamometer must be determined in order to compare the results of one study to another, independent of the type of device used. The purpose of this study was to describe and implement a dynamic calibration test for characterizing the electro-mechanical properties of a dynamometer. The inertia, the viscous friction, the kinetic friction, the motor back-electromotive force constant, and the motor constant were calculated using three different methods. The methodology based on a dynamic calibration test along with a nonlinear regression analysis produced the best results. The coefficient of determination comparing the dynamometer model output to the measured angular velocity and torque was 0.999 for a ramp input and 0.989 for a sinusoidal input. The inertia and resistance were determined for the rollers and the wheelchair wheels. The calculation of the electro-mechanical parameters allows for the complete description of the propulsive torque produced by an individual, given only the angular velocity and acceleration. The measurement of the electro-mechanical properties of the dynamometer as well as the wheelchair/human system provides the information necessary to simulate real-world conditions.

This material is based on work supported by the U.S. Department of Veterans Affairs, Rehabilitation Research and Development Service (B689-RA), and the Paralyzed Veterans of America.

Address all correspondence and requests for reprints to: Rory A. Cooper, PhD, Human Engineering Research Laboratories (151R-1), Center of Excellence for Wheelchairs and Related Technology, VA Pittsburgh Healthcare System, 7180 Highland Drive, Pittsburgh, PA 15206; email: rcooper@pitt.edu.

Key words: *calibration, dynamics, dynamometer, ergometer, wheelchair.*

INTRODUCTION

The study of manual wheelchair propulsion often includes the measurement of physiological, kinematic, and kinetic parameters. The types of devices used in manual wheelchair propulsion studies can be primarily grouped into five categories: a) treadmills (1–3), b) custom-made roller systems (4–6), c) commercially available roller systems (7,8), d) roller systems linked to commercially available bicycle ergometers (9–11), and e) wheelchairs or simulated wheelchairs linked to a custom-made ergometer or dynamometer (12–16). The inertia and resistance components of the device must be determined in order to compare the results of one study to another.

The terms ergometer and dynamometer, often considered interchangeable, are used to describe devices used during stationary manual wheelchair propulsion. An ergometer will be defined as a device that measures work and power only, and has no method of adding power to the system, though it may be able to apply a load. A dynamometer, on the other hand, not only measures work

and power but also measures torque and speed (or position) directly, and has the ability to apply a load or add power to the system.

Calibration of both ergometers and dynamometers is required whether they are custom-built or commercial versions. The calibrations performed by the manufacturer for cycle ergometers have been shown to be in error for mechanically, aerodynamically, and electromagnetically braked ergometers (17–19). The methods used primarily to calibrate an ergometer or dynamometer consist of a dynamic motor-driven test, a deceleration or "coast-down" test, an acceleration test, and a drag test.

The dynamic, motor-driven test consists of using a motor to drive the flywheel or roller at a constant speed while recording speed and torque (4,18,19). This procedure can be repeated at numerous resistance settings, thus providing a table or equation describing the power *versus* speed and resistance setting. This procedure does not provide direct information on the inertia or friction (kinetic friction or viscous friction) inherent in the system. The deceleration or "coast-down" test consists of accelerating the ergometer or dynamometer to a steady-state speed, typically by an individual, and then removing the input and recording speed as a function of time as the device decelerates to zero. Given the inertia of the roller or flywheel and the wheelchair wheel, and the equation that describes speed as a function of time, the friction can be determined. This protocol can be applied to calculate friction while using an ergometer or dynamometer or during a field test (i.e., traversing a floor) (5,20,21). The drag test consists of attaching a load cell between the front of the wheelchair and the frame of the treadmill, running the motor-driven treadmill at different speeds and recording the force, which is the system friction (22). The acceleration test consists of placing the ergometer or dynamometer on a platform (e.g., table or balcony), wrapping a rope or cable around the roller or drive shaft, hanging a weight at the end of the rope, and releasing the weight while the angular acceleration of the roller is recorded. This is repeated with different-sized weights and at different resistance settings. Based on the linear regression of the weight, as a function of the acceleration, the friction and inertia can be determined (17,23). The acceleration test allows for calculation of the inertia of the roller or flywheel used in the device.

The major inaccuracy of the four primary methods used to calibrate an ergometer or dynamometer is the incomplete characterization of the ergometer or dynamometer. None of the previously considered calibration methods separate the friction into a kinetic friction and a viscous (i.e., speed-dependent) friction. Furthermore, only the acceleration test provides a method for directly determining the inertia of the system. Otherwise, inertia is calculated based on the known material properties and geometries of the dynamometer or ergometer.

The incomplete characterization of the ergometer or dynamometer can cause inaccuracies in data reporting in two ways. The first is due to assuming system friction is only dependent on kinetic friction. That is, the viscous friction is negligible or the overall friction is constant across all velocities. With this assumption, power can be easily calculated with changes in velocity rather than changing the resistance setting. The ability to change power based on a change in speed is especially important during field tests (i.e., traversing a floor), where there are no resistance settings. The problem with this is that friction really is not constant across all velocities. Errors are introduced since, as the velocity increases, the torque also increases; however, if this is not accounted for the power calculations will be underestimated. Likewise, if the velocity decreases in order to decrease the power, the power calculations will be overestimated.

The second inaccuracy is due to the assumption that the velocity of manual wheelchair propulsion is constant. This can lead to erroneous results by the fact that two individuals can propel their wheelchairs at the same average velocity, thereby producing the same power, based on power calculations that assume the velocity is constant. In reality, velocity is not constant during manual wheelchair propulsion; so, although the individuals may have significantly different stroke patterns, one much more efficient than the other, this will not be apparent when a constant velocity is assumed. For example, the person with the inefficient propulsion style may have a very jerky stroke with large accelerations, thereby producing a much higher power. The only way this will manifest is if the inertia is known and the acceleration data are included when power is calculated.

This same error also arises when the inertia of the system is not included when reporting biomechanical or physiological parameters measured during manual wheelchair propulsion. Errors arise in the calculation of the torque and power because a constant velocity must be assumed. Furthermore, errors will arise when other researchers want to validate the results of the study, since there is no way to determine if the dynamometer accu-

rately matched the inertia of the individual or a 50th-percentile or 95th-percentile manikin.

Models describing manual wheelchair propulsion on a dynamometer have been developed by several investigators, including Cooper (6,24,25), Hofstad and Patterson (26), Niesing et al. (14), van der Woude et al. (22), and Theisen, Francaux, and Fayt (5). The model described by Cooper (24) was selected because it separates the frictional losses into two components, the viscous friction, which is velocity dependent, and the kinetic friction.

The dynamometer was represented as an electromechanical system (27). The mechanical portion describes the roller characteristics, which are inertia, kinetic friction, and viscous friction, whereas the electronic portion describes the direct current (dc) motor characteristics, which include the back-electromotive force (emf) constant and the motor constant.

The purpose of this study was to describe a dynamic calibration test to characterize a wheelchair dynamometer. The parameters of the system that were addressed are the inertia (J), the viscous friction (B), the kinetic friction (T), the motor back-emf constant (K_b), and the motor constant (κ). Once these parameters were calculated, application of the model to different inputs and comparison of the calculated values to measured values was used for validation.

METHODS

Dynamometer

The dynamometer used in this study consists of two independent, steel tubular rollers, one for each wheel, supported by pillow-block bearings (see **Figures 1** and **2**). The bearings are mounted on a piece of steel channel (1.57 m $\times$ 0.305 m $\times$ 0.762 m) with four adjustable feet (ball and screw) for leveling. Attached to the channel is a frame of steel angle, on which the motors (2,400 rpm, Electro Craft Motor, #703-06-078), torque sensors and speed sensors are mounted (one motor, torque sensor, and speed sensor for each roller). Specially designed stinger-type torque sensors with Wheatstone strain gage bridges (Micromeasurements, 350) were mounted to each dc motor housing. Two tachogenerators were mounted on the frame attached to the rollers. Contact between the roller and the armature of the tachogenerator was maintained using a spring-loaded mount and a rubber roller.

Figure 1.
Wheelchair with SMART^{Wheels} attached to the wheelchair dynamometer.

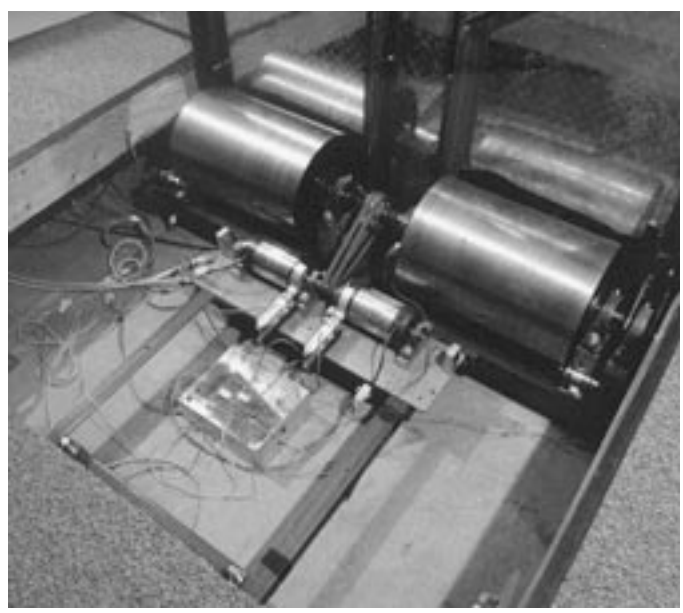

Figure 2.
Wheelchair dynamometer with the platform removed to display the rollers, motors, bearings, tachogenerators, and torque sensors.

The torque and speed data were sampled at 240 Hz, with 8-bit analog-to-digital (A/D) conversion. The torque data were filtered at 40 Hz before A/D conversion. Two

Journal of Rehabilitation Research and Development Vol. 38 No. 1 2001

armature-controlled permanent magnet dc motors were used to provide power to the system in assist mode and mechanical resistance in generator mode. A personal computer, connected to two programmable power supplies (Hewlett Packard HP-IB DC Power Supply, Model 6673A) and two programmable electronic loads (Hewlett Packard HP Electronic Load, Model 6060B) through a general purpose interface bus (GPIB) (National Instruments PCI-GPIB), controlled the dynamometer. Visual Basic was used to create the program that controlled the power supplies and loads.

Model

The model used in this analysis was a combination of a reduced version of Cooper's dynamometer model (24) and an electric motor-load system model (27). A diagram of the wheelchair and dynamometer system is shown in **Figure 3**. **Figure 4a** depicts the Laplace transform block diagram with the armature angular velocity as the output, whereas **Figure 4b** depicts the Laplace transform block diagram with the torque measured at the motor housing as the output.

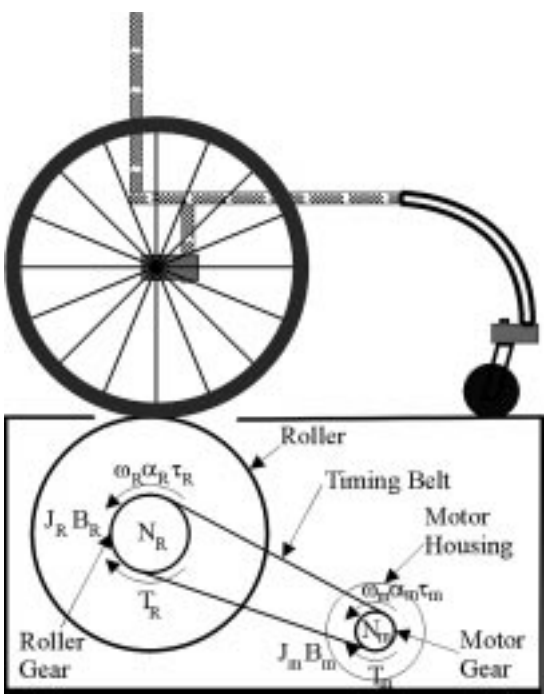

Figure 3.
Diagram of the dynamometer and wheelchair. J, rotational inertia; B, rotational viscous coefficient of friction; T, magnitude of kinetic friction; N, number of gear teeth (note $\beta=N_{R-M}$); ω, angular velocity; α, angular acceleration; τ, torque. R subscript on terms denotes the roller; m subscript denotes the motor.

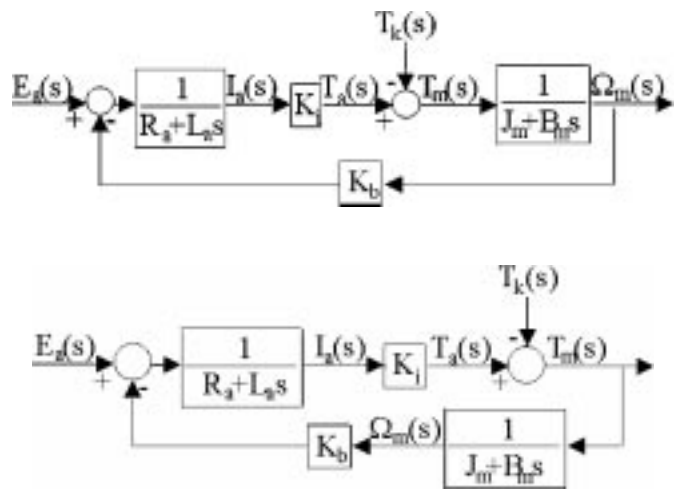

Figure 4.
Block diagram of the dynamometer in the Laplace domain with the voltage across the motor armature, $E_a(s)$ and the kinetic friction, $T_k(s)$, as inputs, and (a) the motor angular velocity, $_m(s)$, and (b)motor torque, $T_m(s)$, as the output. B_m, viscous coefficient of the motor; J_m, motor inertia; K_b, back-emf constant; K_i, motor torque constant; L_a, motor armature inductance; R_a, motor armature resistance; $I_a(s)$, current applied to the armature; $T_a(s)$, torque at the armature; s, Laplace domain operator.

The definitions of the variables and parameters are listed in **Tables 1** and **2**. The motor inductance (L_a) was negligible for our dc motors (28); therefore, the parameter κ, which relates the input voltage (e_a) to the torque generated by the armature (τ_a), can be introduced to further simplify the model (see Equation 1, below).

$$\kappa = \frac{K_i}{R_a} \qquad [1]$$

The characteristic equations for the motor angular velocity and the motor torque in the Laplace domain are given by Equations 2 and 3, respectively.

$$_m(s) = \frac{E_a(s)*\kappa - T_k(s)}{J_{sys,m}} * \frac{1}{s + \frac{B_{sys,m} + K_b*\kappa}{J_{sys,m}}} \qquad [2]$$

$$T_m(s)=[E_a(s)*\kappa - T_k(s)]* \frac{s + \frac{B_{sys,m}}{J_{sys,m}}}{s+\frac{B_{sus,m}+K_b*\kappa}{J_{sys,m}}} \qquad [3]$$

Table 1.
List of variables. Note that the time domain variables are in lower case and the Laplace domain variables are in upper case.

Time Domain	Laplace Domain	Definition
$e_a(t)$	$E_a(s)$	Input Voltage across the armature of the dc motor (V)
$i_a(t)$	$I_a(s)$	Current applied to the armature (A)
$\tau_a(t$	$T_a(s)$	Torque at the armature (N*m)
$\tau_m(t)$	$T_m(s)$	Torque at the motor housing (N*m)
$\tau_k(t)$	$T_k(s)$	Kinetic friction modeled as a disturbance to the system (N*m)
$\tau_W(t)$	$T_W(s)$	Torque at the wheelchair rear wheel (N*m)
$\omega_m(t)$	$_m(s)$	Angular velocity at motor armature (rad/s)
$\omega_R(t)$	$_R(s)$	Angular velocity at roller (rad/s)
$\omega_W(t)$	$_W(s)$	Angular velocity at rear wheel (rad/s)
$\alpha_W(t)$	$A_W(s)$	Angular acceleration at rear wheel (rad/s)

The step voltage input used in the dynamic calibration test is presented in Equation 4, in the Laplace domain where A is the magnitude of the step input voltage.

$$E_a(s) = \frac{A}{s} \qquad [4]$$

The kinetic friction was modeled as a step torque input, Equation 5,

$$T_k(s) = \frac{T_{sys,m}}{s} \qquad [5]$$

where $T_{sys,m}$ is the magnitude of the step torque input in N·m.

Substituting Equations 4 and 5 into Equations 2 and 3, and performing an inverse Laplace transform, produces the model Equations used in the dynamic calibration test, Equations 6 and 7.

In the remainder of the text, the subscript "sys" found in **Equations 2–7** is replaced by either "D" or "D&WC" depending on whether the parameters define values for the dynamometer system only (D) or the dynaometer and wheelchair system (D&WC).

Assuming that the mechanical properties (i.e., rotational inertia, rotational viscous coefficient of friction, and kinetic friction) of the motor are small relative to the roller, then the following equations, Equations 8a, b, c, can be used for the dynamometer system only,
while Equation 9 can be used for the dynamometer and wheelchair system.

The parameters in Equations 8 and 9 are defined in **Table 2**.

Dynamic Calibration Test

The dynamic calibration tests consisted of applying a step-input voltage across the armature of the dc motor and recording the speed and torque with respect to time. The step-input voltage is given by Equation 10, where A was equal to 10 V, 15 V, or 20 V.

$$\omega_m(t) = \frac{A*\kappa - T_{sys,m}}{B_{sys,m} + Kb*\kappa} * \left[1 - exp\left(-\frac{B_{sys,m} + K_b*\kappa}{J_{sys,m}}*t\right)\right] \qquad [6]$$

$$\tau_m(t) = (A*\kappa - T_m)*exp\left(-\frac{B_m + K_b*\kappa}{J_m}*t\right) + \frac{(A*\kappa - T_{sys,m})*B_{sys,m}}{B_{sys,m} + K_b*\kappa} * \left[1 - exp\left(\frac{B_{sys,m} + K_b*\kappa}{J_{sys,m}}*t\right)\right] \qquad [7]$$

$$J_{R,R} \cong J_{D,R}$$
$$B_{R,R} \cong B_{D,R}$$
$$T_{R,R} \cong T_{D,R} \qquad [8]$$

$$J_{w,w} + \beta_{WR}^2 * J_{R,R} \cong J_{D\&WC,W}$$
$$B_{w,w} + \beta_{WR}^2 * B_{R,R} \cong B_{D\&WC,W}$$
$$T_{w,w} + \beta_{WR}^2 * T_{R,R} \cong T_{D\&WC,W} \qquad [9]$$

Table 2.
List of parameters.

Parameter	Definition
A	Magnitude of the step input (V)
$B_{D, R}$	Rotational viscous coefficient of friction of the dynamometer system only reflected at the roller (kg*m^2/s)
$B_{D\&WC, W}$	Rotational viscous coefficient of friction of the dynamometer and wheelchair system reflected at the wheel (kg*m^2/s)
$B_{R, R}$	Rotational viscous coefficient of friction of the roller (kg*m^2/s)
$B_{sys, m}$	System rotational viscous coefficient of friction reflected at the motor (kg*m^2/s)
$B_{W, W}$	Rotational viscous coefficient of friction of the wheel (kg*m^2/s)
C_1-C_6	Coefficients that define the five mechanical and electrical properties of the system. The coefficients are used in conjunction with the linear regression analysis
f	Frequency of the sinusoidal input (Hz)
G	Magnitude of the ramp input (V/s)
$J_{D, R}$	Rotational inertia of the dynamometer system only reflected at the roller (kg*m^2/s)
$J_{D\&WC, W}$	Rotational inertia of the dynamometer system only reflected at the wheel (kg*m^2/s)
$J_{R, R}$	Rotational inertia of the roller (kg*m^2/s)
$J_{sys, m}$	System rotational inertia reflected at the motor (kg*m^2/s)
K_b	Rotational inertia of the wheel (kg*m^2/s)
$J_{D, R}$	Rotational inertia of the dynamometer system only reflected at the roller (kg*m^2/s)
K_b	Back-emf constant (V*s/rad)
K_i	Motor torque constant (N*m/A)
L_a	Motor armature inductance (H)
P	Mechanical Power (W)
Q_1	Magnitude of the offset for the sinusoidal input (V)
Q_2	Amplitude of the sinusoidal input (V)
R_a	Motor armature resistance ( )
R_L	Resistance load--used to simulate different surfaces and grades ( )
R_{eq}	Equilibrium load--used to equate resitance of left and right rollers ( )
$T_{D, R}$	Magnitude of the kinetic friction of the dynamometer system only reflected at the roller (N*m)
$T_{D\&WC, W}$	Magnitude of the kinetic friction of the dynamometer and wheelchair system reflected at the wheel (N*m)
$T_{R, R}$	Magnitude of the roller kinetic friction (N*m)
$T_{sys, m}$	Magnitude of the system kinetic friction at the motor (N*m)
$T_{W, W}$	Magnitude of the wheel kinetic friction (N*m)
β_{Rm}	Ratio of the roller gear diameter to the motor gear diameter
β_{Rm}	Ratio of the wheel gear diameter to the roller gear diameter
κ	Motor constant (N*m/V)

$$e_a(t) = A * u(t) \qquad [10]$$

Ten trials were performed at each voltage, producing 30 trials for each test condition. Four test conditions were implemented in order to describe fully the dynamometer and to examine the sensitivity of the calibration procedure. The first two conditions were the right side dynamometer only (DR) and the left side dynamometer only (DL). The last two conditions consisted of the right side dynamometer with an unoccupied manual wheelchair (D&WCR), and the left side dynamometer with an unoccupied manual wheelchair (D&WCL). SMART^{Wheels} replaced the typical rear mag wheels. The SMART^{Wheel} is a device that allows for the measurement and recording of three-dimensional pushrim forces and moments during dynamic wheelchair propulsion. The SMART^{Wheel} is used in the analysis of manual wheelchair propulsion biomechanics, and is heavier in mass and has a larger inertia than a typical mag wheel, due to the additional weight of the instrumentation required to measure the pushrim forces and moments (29). These four conditions allowed us to investigate the ability of the dynamic calibration test to calculate the mechanical parameters of

not only the dynamometer, but also the mechanical parameters of a wheelchair on the dynamometer, and to compare the symmetry of the dynamometer and wheelchair.

The transient response was defined as 10–90 percent of the final value of the steady-state response. The final value of the steady-state response was defined as the mean of the final 10 percent of the signal of each trial. The start of the steady-state response was defined as 95 percent of the final value for a trial.

The angular velocity and torque data were used in conjunction with a linear regression analysis and nonlinear regression analysis in order to determine the system parameters for each of the four test conditions. Equations 8 and 9 were used with these parameters to identify the dynamic properties of the wheelchair that are pertinent to driving simulation.

Calculation of Model Parameters

Bench-Top Testing

This method consisted of measuring the motor (i.e., electrical) properties separate from the mechanical properties of the dynamometer. The back-emf motor constant, K_b, was calculated from a no load test where K_b is the inverse of the slope of the motor speed as a function of input voltage. The motor constant, κ, was calculated from a stall-torque test where κ is the slope of the motor torque as a function of input voltage. The rotational inertia, $J_{sys,m}$, was calculated based on the known material properties and geometries of the roller and roller shaft. The viscous coefficient of friction, $B_{sys,m}$, and kinetic friction, $T_{sys,m}$, were calculated based on a load test where $B_{sys,m}$ is based on the slope $\times$ κ and $T_{sys,m}$ is based on the y-intercept of the input voltage as a function of speed.

Linear Regression

Linear regressions were performed on the data from the dynamic calibration test in order to determine the system parameters. The coefficients obtained from a linear regression of the motor speed steady-state response as a function of input voltage, Equation 11, and motor-torque steady-state response as a function of input voltage, Equation 12, provide four equations.

$$\lim_{t\to\infty}\omega_m(t) = \frac{A^*\kappa - T_m}{B_m + K_b{}^*\kappa} \qquad [11]$$

$$\lim_{t\to\infty}\tau_m(t) = \frac{B_m{}^*(A^*\kappa - T_m)}{B_m + K_b{}^*\kappa} \qquad [12]$$

Therefore, one more equation is necessary in order to determine all five motor and roller parameters. The transient response of the speed and torque data, Equations 6 and 7, provides two more equations. Upon initial inspection, it may appear that any five of the six equations (based on the six equations obtained from the linear regression analysis) may be selected in order to calculate the five parameters. However, upon further analysis it can be seen that only two sets of equations give explicit solutions for the five parameters.

The appendix provides a complete description of the equations and coefficients used in the linear regression analysis. The linear regressions were performed simultaneously on all 30 trials for a given condition, thereby providing a single result for each parameter.

Nonlinear Regression

A modified Gauss-Newton nonlinear regression (30), in conjunction with Equations 6 and 7, was used to determine all five model parameters simultaneously. The Matlab (The MathWorks, Natick, MA) statistical toolbox package was used to perform the nonlinear regression (31). This method incorporates both the torque and speed data for the entire trial, rather than just the transient or steady-state response, as was done using linear regression. Nonlinear regression requires initial estimates of the parameters, since it is an iterative process. The initial estimates used were those obtained by linear regression.

Following the calculation of the model parameters using the nonlinear regression analysis for the four conditions, the mechanical properties of the rear wheelchair wheel were determined using Equations 8 and 9. The absolute value of the normalized percent difference between the dynamometer and wheelchair system (D&WC) results and the dynamometer only (D) results for the motor parameters, K_b and κ, were calculated using Equation 13.

$$\frac{D\ \&\ WC - D}{D\ \&\ WC + D}\,100\% \qquad [13]$$

Validation of Step Input and Nonlinear Regression to Calibrate Dynamometer

The use of a step input, while recording the armature speed and the torque measured at the motor housing, to calibrate the dynamometer was validated by applying ramp and sinusoidal inputs to the system and comparing the results with the model results. The ramp input is given by Equation 14, where G was equal to 0.5 V/s, 1.0 V/s, or 2.0 V/s.

$$e_a(t) = G * t \quad [14]$$

The sinusoidal input is given by Equation 15, where Q_1 is the offset voltage, 10 V, Q_2 is the amplitude, 5 V, and f is the frequency, 1 Hz, 0.1 Hz, or 0.02 Hz.

$$e_a(t) = Q_1 + Q_2 * \sin(f * t) \quad [15]$$

Ten trials were performed for each ramp input (voltage slope, G) and each sinusoidal input (frequency, f), providing 240 validation trials (6 inputs (3 ramp and 3 sinusoidal) × 10 trials × 4 test conditions (DR, DL, D&WCR, and D&WCL)).

Statistical Analysis

Calibration

For each of the three methods, the coefficient of determination, r_2, was calculated for the transient response, the steady-state response, and the entire trial. For the nonlinear regression, a 95-percent confidence interval for each parameter was determined.

Validation

The r^2 was calculated comparing the measured speed and torque data to the model output data. Only the model parameters from the nonlinear regression analysis were used.

RESULTS

The rotational inertia, rotational viscous coefficient of friction, and kinetic friction of D, as well as the motor back-emf constant and the motor constant, are listed in **Table 3**. The parameters presented in **Table 3** were calculated with nonlinear regression with a 95 percent confidence interval. The measured transient and steady-state responses for the angular velocity and motor torque of the DR condition, given a step voltage input, are displayed in **Figures 5a** and **5b**], respectively, along with the model output data from the nonlinear regression analysis.

Table 3.
The mechanical (J, B, and T) and electrical (K_b and κ) properties of the dynamometer system only, D, and the wheelchair and dynamometer system, D&WC. The mechanical properties are defined by **Equation 8** for the dynamometer system only (rows 2 and 3) and by **Equation 9** for the wheelchair and dynamometer system (rows 4 and 5).

Condition	J (kg*m²/s)	B (kg*m²/s)	T (N*m)	K_b (V*s/rad)	κ (N*m/V)
DR	0.9096±0.0024	0.02440±0.00044	0.7335±0.0034	0.2680±0.0001	0.3684±0.0010
DL	0.9281±0.0032	0.01549±0.00072	0.6595±0.0055	0.2773±0.0002	0.3947±0.0014
D&WCR	3.468±0.009	0.1042±0.0016	1.489±0.007	0.2674±0.0001	0.3672±0.0010
D&WCL	3.557±0.011	0.08668±0.00230	1.085±0.008	0.2551±0.0002	0.3470±0.0010

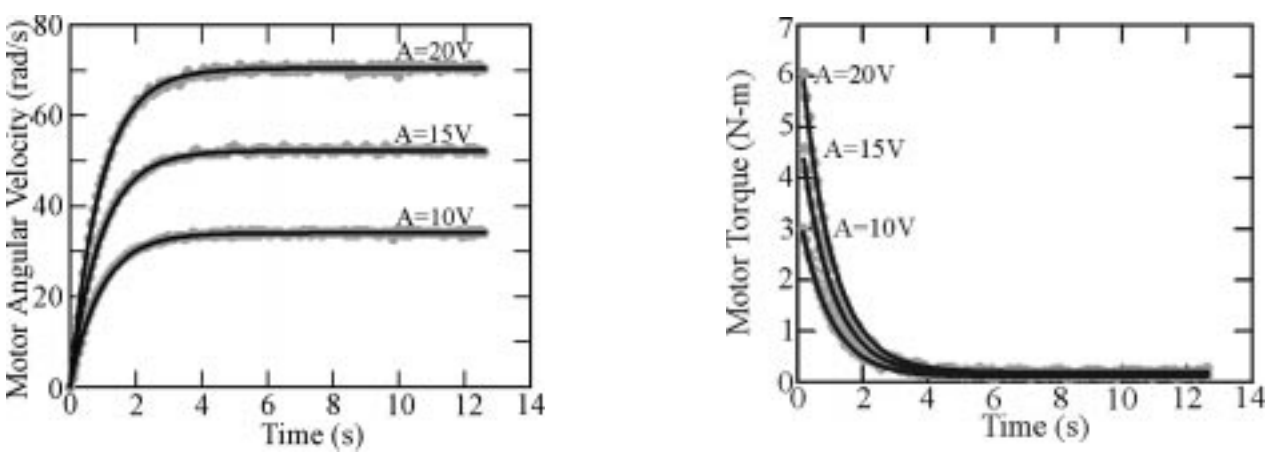

Figure 5.
The measured (O) and calculated (-) transient and steady-state response for the DR condition given a step input, and (a) motor angular velocity, $\omega_m(t)$, and (b) motor torque, $\tau_m(t)$, as the output. The calculated response is based on the parameters obtained from the nonlinear regression analysis of the dynamic calibration test.

The dynamic properties of the rear wheels (i.e., SMART^{Wheels}), listed in **Table 4**, are based on subtracting the results from the D&WC from the results of the D, as described by Equations 8 and 9. The absolute normalized percent difference, Equation 13, between the D&WC results and the D results for K_b are 0.1 percent and 4.2 percent for the right and left sides, respectively, while for κ they are 0.2 percent and 6.4 percent for the right and left sides, respectively.

Note that the absolute normalized percent difference values for the left side were much larger than those for the right. The viscous coefficient of friction for the left SMART^{Wheel} was approximately twice that of the right SMART^{Wheel} and the kinetic friction for the left SMART^{Wheel} was negative. These discrepancies are due to maintenance performed on the left side of the dynamometer during the course of the testing which had the effect of decreasing the overall friction in the system. Specifically, the decrease in the overall friction in the dynamometer due to the maintenance was larger than the increase in friction due to the addition of the SMART^{Wheel}; therefore, the value obtained for the left SMART^{Wheel} kinetic friction is negative. The maintenance consisted of inspecting all bolts and screws, inspecting the wire connections, and removing any grit and dirt from the bearings, which may have accumulated, and lubricating the bearings with a Teflon-based lubricant. The removal of dirt and grit was believed to have decreased the overall friction of the system.

Table 5 compares the coefficient of determination for the angular velocity and torque data obtained from the three analysis methods. The calculated data used to obtain the coefficient of determination were based on the nonlinear regression analysis method (data columns 1–3), the linear regression analysis method (data columns 4–6) and the bench-top testing method (data columns 7–9). The coefficient of determination, r^2, for each of the four conditions (DR, DL, D&WCR, and D&WCL), independent of the type of input voltage (step, ramp, or sinusoidal), was largest for the nonlinear regression analysis (see **Table 5**).

The measured transient and steady-state responses for the motor angular velocity and motor torque of the DR condition, given sinusoidal input at f=0.1Hz, are displayed in **Figures 6a** and **6b** along with the model output data from the nonlinear regression analysis. These figures are typical of all the sinusoidal inputs for all of the four conditions. Since the ramp input r^2 results were larger than the sinusoidal results (**Table 5**), only the sinusoidal input results were depicted.

Table 4.
The mechanical properties of the based on Equations 8 and 9.

SMART^{Wheel}	J_W (kg·m^2)	B_W (kg·m^2/s)	T_W (N·m)
Right	0.1806	0.01604	0.09442
Left	0.2033	0.03071	-0.1685

Table 5.
The coefficient determination, r^2, comparing the measured data to the calculated angular velocity and torque data. The coefficient of determination is the largest for the calculated data based on nonlinear regression (i.e., obtained using the model parameters from the dynamic calibration test) in all cases.

	Coefficient of Determination, r^2								
	Nonlinear Regression			Linear Regression			Bench-Top Testing		
Condition	Step	Ramp	Sinusoidal	Step	Ramp	Sinusoidal	Step	Ramp	Sinusoidal
DR	0.99983	0.99955	0.99722	0.99979	0.99951	0.99682	0.99540	0.99822	0.99556
DL	0.99968	0.99914	0.98958	0.99962	0.99900	0.98857	0.98636	0.99394	0.99577
D&WCR	0.99982	0.99958	0.98825	0.99978	0.99955	0.99795	N/A	N/A	N/A
D&WCL	0.99977	0.99925	0.99878	0.99970	0.99891	0.99862	N/A	N/A	N/A

DR=Right Dynamometer Only, DL=Left Dynamometer Only, D&WCR=Right Dynamometer and Wheelchair, D&WCL=Left Dynamometer and Wheelchair

Journal of Rehabilitation Research and Development Vol. 38 No. 1 2001

DISCUSSION

The nonlinear regression analysis yielded the largest coefficient of determination between the model data and the independent validation data. Nonlinear regression also determines all five model parameters simultaneously, whereas, linear regression and bench-top testing calculate the model parameters independent from each other. Therefore, the linear regression analysis and the bench-top testing do not accurately account for the interaction between parameters. Bench-top testing actually uses four independent tests to determine the parameters, which explains the fact that this method produces the smallest r^2 values. Linear regression is more appropriate than bench-top testing because it uses the angular velocity and torque data from the same trial (transient and steady-state response) to calculate the parameters, rather than data from separate tests. The nonlinear regression produces the best results (**Table 5**) because it uses both the transient and steady-state responses, and the five model parameters are calculated simultaneously.

It might seem that the linear regression analysis is as good a method as the nonlinear regression analysis, since the linear regression analysis also produces large r^2 values (though not as large as the nonlinear regression analysis; see **Table 5**). However, there are three major advantages to implementing the nonlinear regression analysis rather than the linear regression analysis. The first advantage is that a nonlinear regression is specifically intended to calculate the parameters of a nonlinear equation, whereas a linear regression is intended to determine the parameters of a linear equation (e.g., polynomial or intrinsically linear). Given this information, and the fact that **Equations 6** and **7** are nonlinear equations, the nonlinear regression is the most appropriate method to determine the model parameters.

The second advantage of the nonlinear regression is that each individual parameter can be calculated directly, whereas the linear regression calculates the coefficients in each of the terms of Equations 6, 7, 10, and 11. The model parameters are then indirectly calculated based on the coefficients (see Appendix).

The third advantage is that both the transient and steady-state response can be analyzed simultaneously (as a single process) in order to determine the system parameters with the nonlinear regression. Conversely, the linear regression analysis requires the assumption that the transient response is obtained from a different process than the steady-state response, although, in this situation, this is an inappropriate assumption. The recommendation of using the nonlinear regression analysis instead of the linear regression analysis is based on these three advantages as well as the fact that the coefficient of determination is larger for the nonlinear regression.

The parameters calculated using the dynamic calibration test and the nonlinear regression analysis (**Table 3**) resulted in a confidence interval, ±97.5 percent, less than 1 percent of the calculated value. The exception was the rotational viscous coefficient of friction, which is less than 2 percent for the right side and less than 5 percent for

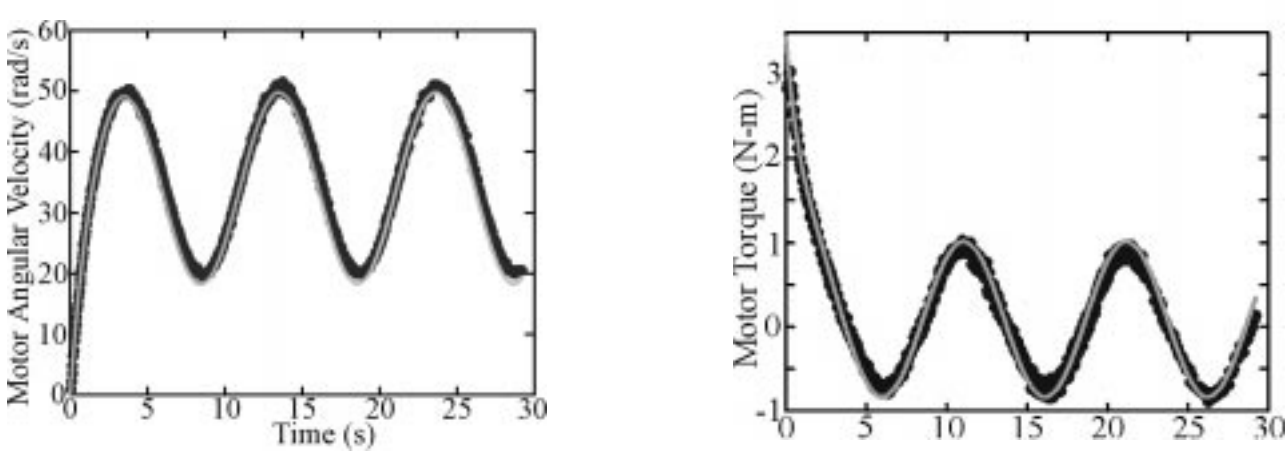

Figure 6.
The measured (O) and calculated (-) transient and steady-state response for the DYNR condition given a sinusoidal input at f=0.1 Hz, and (a) motor angular velocity, $\omega_m(t)$, and (b) motor torque, $\tau_m(t)$, as the output.

the left side. The large r^2 values (data columns 1–3, **Table 5**), obtained when the model output data given a step, ramp or sinusoidal voltage input were compared to the actual data, further suggest that these parameters are accurate. **Figures 5a** and **5b** further indicate the ability of the nonlinear regression to determine the model parameters for the DR condition. This suggests that the nonlinear regression is appropriate for determining the model parameters. **Figures 6a** and **6b** further validate the ability of the model, in conjunction with a dynamic calibration test and nonlinear regression, to accurately represent the data obtained from the ramp and sinusoidal inputs.

Considering the right side of the system only, DR and D&WCR, the normalized difference is less than 0.2 percent for K_b and κ, showing that changes in the mechanical properties of the system do not affect the calculation of the motor constants, as expected. Furthermore, the inertia and coefficients of viscous friction and kinetic friction increase, as expected, from the DR system to the D&WCR system, allowing the direct calculation of these variables for the SMART^{Wheel} (Equations 8 and 9, and **Table 4**).

Considering the left side of the system only, DL and D&WCL, some discrepancies in the expected results arose. As described in the results, these discrepancies are due to maintenance performed on the left side of the dynamometer during the course of testing that had the effect of lowering the overall friction. This affected the calculation of the viscous and kinetic friction for the SMART^{Wheel}. However, it did not affect the accuracy of calculating the rotational inertia of the SMART^{Wheel} (**Table 4**) since the roller inertia was not altered during the maintenance. In certain respects, this can be considered a positive outcome since the dynamic calibration is able to detect small changes in the system's friction. Furthermore, this indicates that the parameters are calculated independent of each other, since this maintenance did not have an effect on the roller inertia. Finally, the effects of the maintenance are still small considering the absolute, normalized percent difference, Equation 13, is less than 7 percent for K_b and κ on the left side.

The calculation of the rotational inertia of the two SMART^{Wheels} (0.3839 kg-m^2) is larger than the value reported by Coutts (0.2638 kg·m^2; reference 20). The SMART^{Wheels} inertia is larger because mag wheels are used instead of spoked wheels and because the SMART^{Wheels} has added components in order to measure the pushrim forces and moments (29). The calculation of the equivalent mass is 75.62 kg based on a rear-wheel radius of 0.3048 m.

The calibrations used for cycle ergometers (17–19,23) and wheelchair ergometers or dynamometers (4–6,9,11,21,32), have concentrated on determining resistance and power. These investigations have included the viscous friction in their measurements, even though not stated explicitly. Previous studies did not consider the viscous friction independent of the kinetic friction in determining the resistance and power, and they typically do not report the inertia of the dynamometer rollers or the wheelchair wheels. It is difficult to compare results without this information, since different speeds, resistances, and/or inertia setups may be used when constructing the methodology of the biomechanical or physiological studies of manual wheelchair propulsion.

Accurately calibrating a dynamometer requires measuring both the viscous friction and kinetic friction, separately, rather than as one lumped parameter. This is because viscous friction is velocity dependent and the kinetic friction is a constant. Simple formulae, assuming constant velocity on the part of the individual propelling the wheelchair, to calculate the resistance at any angular velocity are given in **Equations 16** and **17**. **Equation 16** describes the resistance, given a constant speed and no connection to a generator.

$$\tau_W(t) = B_{D\&WC,W} * \omega_W(t) + T_{D\&WC,W} \qquad [16]$$

The case when a generator is connected to the rollers is presented in Equation 17.

$$\tau_W(t) = \left(K_b * \kappa * \beta_{WR}^2 * \beta_{Rm}^2 + B_{D\&WC,W} \right) * \omega_W(t) + T_{D\&WC,W} \qquad [17]$$

The calculation methods described in previous cycle ergometer and wheelchair ergometer or dynamometer literature are only able to calibrate their system for discrete speeds and resistance settings. Therefore, if an individual propelling a wheelchair is unable to maintain the velocity for which the ergometer or dynamometer is calibrated, another calibration will be required in order to match the velocity of the individual. The method presented in this study allows calculation of resistance for a speed continuum within the calibration range.

The contribution of the viscous friction (i.e., velocity dependent friction) to the overall friction when the rollers are not linked to the dc motors (i.e., friction independent of the motor parameters, see Equation 16) is 14 percent at 0.9 m/s and 25 percent at 1.8 m/s for the D. Furthermore, the contribution of the viscous friction to the total friction for the

D&WC system is 19 percent at 0.9 m/s and 32 percent at 1.8 m/s. Viscous friction makes a substantial contribution to the total friction. The effect of the velocity-dependent resistance becomes more prominent when the motors are connected to the rollers due to the effect of the viscous friction and the combination of the motor constant, κ, and the motor back-emf constant, K_b (see Equation 17). Therefore, it is important to calculate both the viscous friction and the kinetic friction.

Manual-wheelchair propulsion is a cyclic activity resulting in a change in angular velocity with each stroke. It is important to determine the inertial characteristics of the dynamometer as well as to be able to match the inertial properties of each individual. This allows for the determination of the torque required to overcome the inertial properties of the dynamometer and wheelchair system when calculating the overall resistance and power. It also allows for the accurate simulation of the real-world environment. Equation 18 describes the resistance, given a nonzero acceleration and with the dc motors attached to the rollers.

$$\tau_W(t) = J_{D\&WC,W} * \alpha_W(t) + \left(K_b * \kappa * \beta_{WR}^2 * \beta_{Rm}^2 + B_{D\&WC,W}\right) * \omega_W(t) + T_{D\&WC,W} \quad [18]$$

It is important to calculate the inertia of the system if the instantaneous power of the system needs to be determined, or when within-stroke characteristics (e.g., peak torque or change in torque during the propulsion phase) are considered. Within either of these scenarios it is no longer plausible to assume that the angular velocity is constant.

Once the dynamometer is calibrated, it can be used to set up different conditions, either by applying power to the system using a power supply and servo amplifier or by sinking power through the use of an electronic load (**Figure 7**]). Since the majority of research in manual-wheelchair propulsion has applied loads to the ergometer or dynamometer, a simple application of changing the electrical resistance across the armature of the dc motor is described, assuming a constant velocity. The electrical resistances used in this application will be 5 ohms, which simulates (with our dynamometer system) an individual propelling his/her wheelchair uphill, and 1,000 ohms,

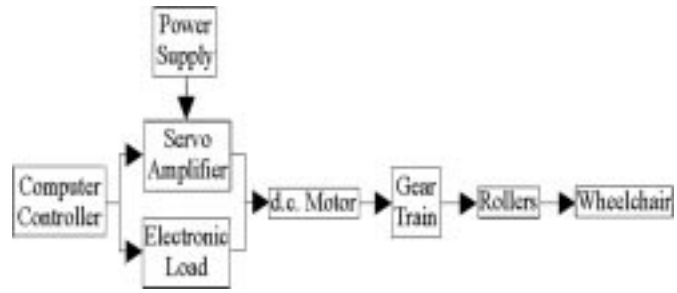

Figure 7.
Functional block diagram of the dynamometer and wheelchair. Only the power supply and servo amplifier are used during the dynamic calibration test. The electronic load, power supply and servo amplifier are incorporated for the simulation of real world conditions.

which simulates an individual propelling his/her wheelchair on a level surface (33). It is important to note that the servo amplifier and power supply are not incorporated into this example application.

Due to differences in the right and left sides of the system, the first step is to determine the load resistance required to equate the two sides, R_{eq}, given that the velocity is constant and equivalent for both sides. Using Equation 17, and setting torque at the right rear wheel ($\tau_{W\text{-right}}$) equal to torque at the left rear wheel ($\tau_{W\text{-left}}$), gives Equation 19.

The equilibrium resistance is dependent on the angular velocity at which the individual will propel the wheelchair. Given the values in rows 4 and 5 of **Table 3**, $R_{L\text{-left}}$ is set to 0.0, K_i is equal to 0.2824 N·m/A (per dc motor-manufacturer specifications) and $R_{L\text{-right}}$ can be redefined as the equilibrium resistance R_{eq}, the electronic load connected to the right motor should apply a resistance of 0.13 ohms for a constant velocity of 0.9 m/s and 0.11 ohms for a constant velocity of 1.8 m/s.

$$\kappa_{left} = \frac{K_i}{R_{a-left} + R_{L-left}} \quad \kappa_{right} = \frac{K_i}{R_{a-right} + R_{L-right}}$$

Once R_{eq} is determined, the power that is generated at different speeds with different loads can be determined using **Equations 20** and **21**.

$$R_{eq} = \left[\frac{K_{b-left} * \beta_{Rm} * \beta_{WR}}{R_{a-left} + R_{L-left}} + \frac{\omega_W * \left(B_{D\&WC,W-left} - B_{D\&WC,W-right}\right) + T_{D\&WC,W-left} - T_{D\&WC,W-right}}{K_i * \beta_{Rm} * \beta_{WR} * \omega_W}\right]^{-1} * K_{b-right} * \beta_{Rm} * \beta_{WR} - R_{a-right} \quad [19]$$

$$\tau(t) = \left[B_{D\&WC,W-left} + B_{D\&WC,W-right} + K_i * \beta_{Rm} * \beta_{WR} * \left(\frac{K_{b-left} * \beta_{Rm} * \beta_{WR}}{R_{a-left} + R_{L-left} + R_{eq}} + \frac{K_{b-right} * \beta_{Rm} * \beta_{WR}}{R_{a-right} + R_{L-right}} \right) \right] * \omega_W(t) + T_{D\&WC,W-left} + T_{D\&WC,W-right} \quad [20]$$

$$P(t) = \tau(t) * \omega_W(t) \quad [21]$$

Given the parameters in rows 4 and 5 of **Table 3**, and examining the cases when $R_{L\text{-left}}=R_{L\text{-right}}$ is equal to 0 ohms, 5 ohms, and 1,000 ohms, and R_{eq} is equal to 0.13 ohms at 0.9 m/s and 0.11 ohms at 1.8 m/s, produces power values as described in **Table 6**.

Therefore, different power settings can easily be set and recorded given **Equations 20** and **21**, R_{eq}, and a constant velocity. The use of **Equation 18** is more appropriate than using the torque data measured via the torque sensors, because the torque sensors do not measure the torque required to overcome the frictions in the system.

In a clinical setting the dynamometer can be calibrated using typical-wheelchair or multiple-wheelchair styles in conjunction with a 50th- or 95th- percentile dummy. This calibration procedure is only appropriate when exercise, conditioning, or diagnostic testing are the primary purpose of the dynamometer; constant velocity may be assumed; and exact matching of the inertia is not necessary. In a research setting, where exact calibration of the dynamometer is required, the methodology could be applied for each individual and his/her wheelchair before the start of the experiment. The viscous and kinetic frictions, inertia, and motor properties can be reported for each test condition.

The accurate calculation of system parameters is important in order to create a dynamometer that simulates real-world conditions (e.g., inertia matching or simulating multiple-surface conditions through the implementation of a feedback control system), and in order to accurately describe the system when reporting results. This allows for accurate comparisons of prior and future data, whether it is physiological, kinetic, or kinematic. The calibration process, based on the authors' experience, would require 10–15 min. Assuming the input step voltage is very consistent from trial to trial, only three to five trials are necessary to calibrate the dynamometer. Given that each trial requires approximately 1 min to perform and that it takes approximately 5–10 min to perform the analysis, the entire procedure should only take 10–15 min.

CONCLUSION

Nonlinear regression analysis of the velocity and torque data provides a validated method for determining the electro-mechanical parameters of a wheelchair dynamometer. Engineers and researchers can use this methodology to set up a protocol for exercise or biomechanical testing, whether it is for training purposes or diagnostic purposes. Through the application of an electronic load and a power supply, a variety of real-world conditions can be simulated, such as propelling a wheelchair on a graded surface, on different types of surfaces, on a turn or straightaway, or on a side slope.

Table 6.
Calculated power output produced given the D&WC system when an individual propels his/her wheelchair using equations (18) and (19). The angular velocity is assumed to be constant. The resistance load of 5 simulates an uphill surface and of 1000 simulates a level surface. The resistance load of 0 is used for comparison purposes only.

	Power (W)		
Wheel Angular Velocity (m/s)	$R_L = 0$	$R_L = 5$	$R_L = 1000$
0.89	60.80	16.73	9.24
1.79	230.33	51.83	21.85

Journal of Rehabilitation Research and Development Vol. 38 No. 1 2001

APPENDIX

CALCULATION OF MODEL PARAMETERS BASED ON A LINEAR REGRESSION

The steady-state equations (Equations 10 and 11) can be rewritten as

$$\lim_{t\to\infty}\omega_m(t) = C_1 * A - C_2 \qquad [A1]$$

$$\lim_{t\to\infty}\tau_m(t) = C_3 * A - C_4 \qquad [A2]$$

where A is the magnitude of the step input in volts and the equations describing the coefficients, C_1 through C_e follow,

$$C_1 = \frac{\kappa}{B_m + K_b * \kappa} \qquad [A3]$$

$$C_2 = \frac{T_m}{B_m + K_b * \kappa} \qquad [A4]$$

$$C_3 = \frac{B_m * \kappa}{B_m + K_b * \kappa} \qquad [A5]$$

$$C_4 = \frac{B_m * T_m}{B_m + K_b * \kappa} \qquad [A6]$$

thus providing four equations for the five unknown parameters. Therefore, at least one more independent coefficient (i.e., equation) is required to solve for the five unknown parameters. Using the results from the linear regression analysis of the steady-state response and performing a logarithmic transformation on the transient equations, Equations 6 and 7 can be rewritten as

$$\omega_m(t) = (C_1 * A - C_2) * [1 - \exp(-C_5 * t)] \qquad [A7]$$

$$\tau_m(t) = C_6 * \exp(-C_5 * t) + C_3 * A - C_4 \qquad [A8]$$

where the equations describing the coefficients, C_5 and C_6, are as follows:

$$C_5 = \frac{B_m + K_b * \kappa}{J_m} \qquad [A9]$$

$$C_6 (A * \kappa - T_m) * \left(1 - \frac{B_m}{B_m + K_b * \kappa}\right) \qquad [A10]$$

Upon initial inspection, it might appear that any five of the six equations describing the coefficients may be selected in order to calculate the five parameters. However, upon further analysis it can be seen that only two sets of equations give explicit solutions. The two sets are (A3, A5, A6, A9, A10) and (A3, A4, A5, A9, A10). Note that this method assumes that the transient and steady-state responses are obtained from two independent processes; however, they are obtained from the same process. This is a weakness of the linear-regression analysis.

REFERENCES

1. Veeger HEJ, van der Woude LHV, Rozendal RH. A computerized wheelchair ergometer. Scand J Rehabil Med 1992;24:17–23.
2. van der Woude LHV, Hendrich KMM, Veeger HEJ, van Ingen Schenau GJ, Rozendal RH, de Groot G, Hollander AP. Manual wheelchair propulsion: effects of power output on physiology and technique. Med Sci Sports Exerc 1988;20:70–8.
3. Hartung GH, Lally DA, Blancq RJ. Comparison of treadmill exercise testing protocols for wheelchair users. Eur J Appl Physiol 1999;66:362–5.
4. Langbein WE, Robinson CJ, Kynast L, Fehr L. Calibration of a new wheelchair ergometer: the wheelchair aerobic fitness trainer. IEEE Trans Rehabil Eng 1993;1:49–58.
5. Theisen D, Francaux M, Fayt A. A new procedure to determine external power output during handrim wheelchair propulsion on a roller ergometer: a reliability study. Int J Sports Med 1996;17:564–71.
6. Cooper RA, Fletcher-Shaw TL, Robertson RN. Model reference adaptive control of heart rate during wheelchair ergometry. IEEE Trans Control Sys Tech 1998;6:307–14.
7. Schmid A, Huonker M, Stober P, Barturen J, Schmidt-Trucksäss A, Dürr H, et al. Physical performance and cardiovascular and metabolic adaptation of elite female wheelchair basketball players in wheelchair ergometry and in competition. Am J Phys Med Rehabil 1998;77:527–33.
8. Wang YT, Deutsch H, Morse M, Hedrick B, Millikan T. Three-dimensional kinematics of wheelchair propulsion across racing speeds. Adapt Phys Activ Qrtr 1995;12:78–89.
9. Newsam CJ, Mulroy SJ, Gronley J, Bontrager EL, Perry J. Temporal-spatial characteristics of wheelchair propulsion: effects of level of spinal cord injury, terrain, and propulsion rate. Am J Phys Med Rehabil 1996;75:292–9.

10. Linden AL, Holland GJ, Loy SF, Vincent WJ. A physiological comparison of forward *versus* reverse wheelchair ergometry. Med Sci Sports Exerc 1999;25:1265–8.
11. Forchheimer F, Lundberg Å. Wheelchair ergometer. Scand J Rehabil Med 1986;18:59–63.
12. Jarvis S, Rolfe H. The use of an inertial dynamometer to explore the design of children's wheelchairs. Scand J Rehabil Med 1982;14:167–76.
13. Keyser RE, Rodgers MM, Gardner ER, Russell PJ. Oxygen uptake during peak graded exercise and single-stage fatigue tests of wheelchair propulsion in manual wheelchair users and the able-bodied. Arch Phys Med Rehabil 1999;80:1288–92.
14. Niesing R, Eijskoot F, Kranse R, den Ouden AH, Storm J, Veeger HEJ, et al. Computer-controlled wheelchair ergometer. Med Biol Eng Comput 1990;28:329–38.
15. Burkett LN, Chisum J, Cook R, Norton B, Taylor B, Ruppert K, Wells C. Construction and validation of a hysteresis brake wheelchair ergometer. Adapt Phys Activ Qrtr 1987;4:60–71.
16. Pará G, Noreau L, Simard C. Prediction of maximal aerobic power from a submaximal exercise test performed by paraplegics on a wheelchair ergometer. Paraplegia 1993;31:584–92.
17. Van Praagh E, Bedu M, Roddier P, Coudert J. A simple calibration method for mechanically braked cycle ergometers. Int J Sports Med 1992;13:27–30.
18. Woods GF, Day L, Withers RT, Ilsley AH, Maxwell BF. The dynamic calibration of cycle ergometers. Int J Sports Med 1994;15:168–71.
19. Maxwell BF, Withers RT, Ilsley AH, Wakim MJ, Woods GF, Day L. Dynamic calibration of mechanically, air- and electromagnetically braked cycle ergometers. Eur J Appl Physiol 1998;78:346–52.
20. Coutts KD. Dynamic characteristics of a sport wheelchair. J Rehabil Res Dev 1991;28:45–50.
21. DiGiovine CP, Cooper RA, Dvorznak MJ. Modeling and analysis of a manual wheelchair coast down protocol. Proceedings of the 19th Annual International Conference of the IEEE Engineering in Medicine and Biology Society; 1997 Oct 29–Nov 2, Chicago, IL; 1997. p. 1888–91.
22. van der Woude LHV, de Groot G, Hollander AP, van Ingen Schenau GJ, Rozendal RH. Wheelchair ergonomics and physiological testing of prototypes. Ergonomics 1999;29:1561–73.
23. Coleman SGS, Hale T. The effect of different calculation methods of flywheel parameters on the wingate anaerobic test. Can J Appl Physiol 1998;23:409–17.
24. Cooper RA. A systems approach to the modeling of racing wheelchair propulsion. J Rehabil Res Dev 1990;27:151–62.
25. Cooper RA. A force/energy optimization model for wheelchair athletics. IEEE Trans Syst Man Cyber 1990;20:444–9.
26. Hofstad M, Patterson PE. Modelling the propulsion characteristics of a standard wheelchair. J Rehabil Res Dev 1994;31:129–37.
27. Kuo BC. Automatic control systems. Englewood Cliffs, NJ: Prentice Hall; 1991. p. 123–202.
28. Nise NS. Control systems engineering. Redwood City, CA: Bejamin/Cummings Publishing Co.; 1995. p. 20–6.
29. Asato KT, Cooper RA, Robertson RN, Ster JF. SMART^{Wheels}: development and testing of a system for measuring manual wheelchair propulsion dynamics. IEEE Trans Biomed Eng 1993;40:1320–4.
30. Gallant AR. Nonlinear statistical models. New York: Wiley; 1987. p. 1–77.
31. MATLAB. Version 5.1.0.421. Natick (MA): The MathWorks, Inc.; 1997.
32. Goosey VL, Campbell IG. Symmetry of the elbow kinematics during racing wheelchair propulsion. Ergonomics 1998;41:1810–20.
33. O'Connor TJ, DiGiovine MM, Cooper RA, DiGiovine CP, Boninger ML. Comparing a prototype geared pushrim and standard manual wheelchair pushrim using physiological data. Saudi J Disabil Rehabil 1998;4:215–23.

Submitted for publication March 10, 2000. Accepted in revised form July 12, 2000.